


## SHORT COMMUNICATION

# Solar cell efficiency tables (Version 61)

Martin A. Green<sup>1</sup>  | Ewan D. Dunlop<sup>2</sup> | Gerald Siefer<sup>3</sup> | Masahiro Yoshita<sup>4</sup> | Nikos Kopidakis<sup>5</sup> | Karsten Bothe<sup>6</sup> | Xiaojing Hao<sup>1</sup>

<sup>1</sup>Australian Centre for Advanced Photovoltaics, School of Photovoltaic and Renewable Energy Engineering, University of New South Wales, Sydney, Australia

<sup>2</sup>Joint Research Centre, European Commission, Ispra, Italy

<sup>3</sup>Fraunhofer-Institute for Solar Energy Systems - ISE CalLab, Freiburg, Germany

<sup>4</sup>Renewable Energy Research Center (RENRC), National Institute of Advanced Industrial Science and Technology (AIST), Ibaraki, Japan

<sup>5</sup>National Renewable Energy Laboratory, Golden, Colorado, USA

<sup>6</sup>Calibration and Test Center, Solar Cells Laboratory, Institut für Solarenergieforschung GmbH (ISFH), Emmerthal, Germany

## Correspondence

Martin A. Green, School of Photovoltaic and Renewable Energy Engineering, University of New South Wales, Sydney, 2052, Australia.  
Email: [m.green@unsw.edu.au](mailto:m.green@unsw.edu.au)

## Funding information

Australian Renewable Energy Agency; U.S. Department of Energy (Office of Science, Office of Basic Energy Sciences and Energy Efficiency and Renewable Energy, Solar Energy Technology Program); Japanese New Energy and Industrial Technology Development Organisation

## Abstract

Consolidated tables showing an extensive listing of the highest independently confirmed efficiencies for solar cells and modules are presented. Guidelines for inclusion of results into these tables are outlined, and new entries since July 2022 are reviewed. Graphs showing progress with each cell technology over the 30-year history of the tables are also included plus an updated list of designated test centres.

## KEYWORDS

energy conversion efficiency, photovoltaic efficiency, solar cell efficiency

## 1 | INTRODUCTION

Since January 1993, *Progress in Photovoltaics* has published six monthly listings of the highest confirmed efficiencies for a range of photovoltaic cell and module technologies.<sup>1,2</sup> By providing guidelines for inclusion of results into these tables, this not only provides an authoritative summary of the current state-of-the-art but also encourages researchers to seek independent confirmation of results and to report results on a standardised basis. In Version 33 of these tables,<sup>2</sup> results were updated to the new internationally accepted reference spectrum (International Electrotechnical Commission IEC 60904-3, Ed. 2, 2008).

The most important criterion for inclusion of results into the tables is that they must have been independently measured by a recognised test centre listed in Appendix A. A distinction is made

between three different eligible definitions of cell area: total area, aperture area and designated illumination area, as defined in Appendix B (note that, if masking is used, masks must have a simple aperture geometry, such as square, rectangular or circular—masks with multiple openings are not eligible). “Active area” efficiencies are not included. There are also certain minimum values of the area sought for the different device types (above 0.05 cm<sup>2</sup> for a concentrator cell, 1 cm<sup>2</sup> for a one-sun cell, 200 cm<sup>2</sup> for a “submodule” and 800 cm<sup>2</sup> for a module).

In recent years, approaches for contacting large-area solar cells during measurement have become increasingly complex. Since there is no explicit standard for the design of solar cell contacting units, in Appendix A of the previous issue,<sup>1</sup> we describe approaches for temporary electrical contacting of large-area solar cells with and without busbars. To enable comparability between different contacting

This is an open access article under the terms of the [Creative Commons Attribution-NonCommercial-NoDerivs](https://creativecommons.org/licenses/by-nc-nd/4.0/) License, which permits use and distribution in any medium, provided the original work is properly cited, the use is non-commercial and no modifications or adaptations are made.

© 2022 The Authors. *Progress in Photovoltaics: Research and Applications* published by John Wiley & Sons Ltd.

**TABLE 1** Confirmed single-junction terrestrial cell and submodule efficiencies measured under the global AM1.5 spectrum (1000 W/m<sup>2</sup>) at 25°C (IEC 60904-3: 2008 or ASTM G-173-03 global)

Classification	Efficiency (%)	Area (cm <sup>2</sup> )	V <sub>oc</sub> (V)	J <sub>sc</sub> (mA/cm <sup>2</sup> )	Fill factor (%)	Test centre (date)	Description
<i>Silicon</i>							
Si (crystalline cell)	26.8 ± 0.4 <sup>a</sup>	274.4 (t)	0.7514	41.45 <sup>b</sup>	86.1	ISFH (10/22)	LONGi, n-type HJT <sup>3</sup>
Si (DS wafer cell)	24.4 ± 0.3 <sup>a</sup>	267.5 (t)	0.7132	41.47 <sup>c</sup>	82.5	ISFH (8/20)	Jinko Solar, n-type
Si (thin transfer submodule)	21.2 ± 0.4	239.7 (ap)	0.687 <sup>d</sup>	38.50 <sup>d,e</sup>	80.3	NREL (4/14)	Solexel (35 µm thick) <sup>4</sup>
Si (thin film minimodule)	10.5 ± 0.3	94.0 (ap)	0.492 <sup>d</sup>	29.7 <sup>d,f</sup>	72.1	FhG-ISE (8/07)	CSG Solar (<2 µm on glass) <sup>5</sup>
<i>III-V Cells</i>							
GaAs (thin film cell)	29.1 ± 0.6	0.998 (ap)	1.1272	29.78 <sup>g</sup>	86.7	FhG-ISE (10/18)	Alta Devices <sup>6</sup>
GaAs (multicrystalline)	18.4 ± 0.5	4.011 (t)	0.994	23.2	79.7	NREL (11/95)	RTI, Ge substrate <sup>7</sup>
InP (crystalline cell)	24.2 ± 0.5 <sup>h</sup>	1.008 (ap)	0.939	31.15 <sup>i</sup>	82.6	NREL (3/13)	NREL <sup>8</sup>
<i>Thin Film Chalcogenide</i>							
CIGS (cell) (Cd-free)	23.35 ± 0.5	1.043 (da)	0.734	39.58 <sup>j</sup>	80.4	AIST (11/18)	Solar Frontier <sup>9</sup>
CIGSSe (submodule)	19.8 ± 0.5	665.4 (ap)	0.688	37.96 <sup>k</sup>	75.9	NREL (12/21)	Avancis, 110 cells <sup>10</sup>
CdTe (cell)	21.0 ± 0.4	1.0623 (ap)	0.8759	30.25 <sup>e</sup>	79.4	Newport (8/14)	First Solar, on glass <sup>11</sup>
CZTSSe (cell)	11.3 ± 0.3	1.1761 (da)	0.5333	33.57 <sup>g</sup>	63.0	Newport (10/18)	DGIST, Korea <sup>12</sup>
CZTS (cell)	10.0 ± 0.2	1.113 (da)	0.7083	21.77 <sup>i</sup>	65.1	NREL (3/17)	UNSW <sup>13</sup>
<i>Amorphous/Microcrystalline</i>							
Si (amorphous cell)	10.2 ± 0.3 <sup>l,h</sup>	1.001 (da)	0.896	16.36 <sup>e</sup>	69.8	AIST (7/14)	AIST <sup>14</sup>
Si (microcrystalline cell)	11.9 ± 0.3 <sup>h</sup>	1.044 (da)	0.550	29.72 <sup>i</sup>	75.0	AIST (2/17)	AIST <sup>15</sup>
<i>Perovskite</i>							
Perovskite (cell)	23.7 ± 0.5 <sup>m</sup>	1.062 (da)	1.213	24.99 <sup>k</sup>	78.4	NPVM (5/22)	U.Sci.Tech., Hefei <sup>16</sup>
Perovskite (minimodule)	22.4 ± 0.5 <sup>m</sup>	26.02 (da)	1.127 <sup>d</sup>	25.61 <sup>d,b</sup>	77.6	NPVM (7/22)	EPFLSion/NCEPU, 8 cells <sup>17</sup>
<i>Dye sensitised</i>							
Dye (cell)	11.9 ± 0.4 <sup>n</sup>	1.005 (da)	0.744	22.47 <sup>o</sup>	71.2	AIST (9/12)	Sharp <sup>18,19</sup>
Dye (minimodule)	10.7 ± 0.4 <sup>n</sup>	26.55 (da)	0.754 <sup>d</sup>	20.19 <sup>d,p</sup>	69.9	AIST (2/15)	Sharp, 7 serial cells <sup>18,19</sup>
Dye (submodule)	8.8 ± 0.3 <sup>n</sup>	398.8 (da)	0.697 <sup>d</sup>	18.42 <sup>d,q</sup>	68.7	AIST (9/12)	Sharp, 26 serial cells <sup>18,19</sup>
<i>Organic</i>							
Organic (cell)	15.2 ± 0.2 <sup>h,r</sup>	1.015 (da)	0.8467	24.24 <sup>c</sup>	74.3	FhG-ISE (10/20)	Fraunhofer ISE <sup>20</sup>
Organic (minimodule)	14.5 ± 0.3 <sup>r</sup>	19.31 (da)	0.8518 <sup>d</sup>	23.51 <sup>d,k</sup>	72.5	JET (12/21)	ZJU/Microquanta, 7 cells <sup>21</sup>
Organic (submodule)	11.7 ± 0.2 <sup>r</sup>	203.98 (da)	0.8177 <sup>d</sup>	20.68 <sup>d,s</sup>	69.3	FhG-ISE (10/19)	ZAE Bayern, 33 cells <sup>22</sup>

Abbreviations: (ap), aperture area; AIST, Japanese National Institute of Advanced Industrial Science and Technology; a-Si, amorphous silicon/hydrogen alloy; CIGS, CuIn<sub>1-y</sub>Ga<sub>y</sub>Se<sub>2</sub>; CZTS, Cu<sub>2</sub>ZnSnS<sub>4</sub>; CZTSSe, Cu<sub>2</sub>ZnSnS<sub>4-y</sub>Se<sub>y</sub>; (da), designated illumination area; DS, directionally solidified (including mono cast and multicrystalline); FhG-ISE, Fraunhofer Institut für Solare Energiesysteme; nc-Si, nanocrystalline or microcrystalline silicon; (t), total area.

<sup>a</sup>Contacting: front: 9BB, busbar resistance neglecting; rear: 9BB, full area contacting, highly reflective chuck.

<sup>b</sup>Spectral response and current–voltage curve reported in present version of these tables.

<sup>c</sup>Spectral response and current–voltage curve reported in Version 57 of these tables.

<sup>d</sup>Reported on a “per cell” basis.

<sup>e</sup>Spectral responses and current–voltage curve reported in Version 45 of these tables.

<sup>f</sup>Recalibrated from original measurement.

<sup>g</sup>Spectral response and current–voltage curve reported in Version 53 of these tables.

<sup>h</sup>Not measured at an external laboratory.

<sup>i</sup>Spectral response and current–voltage curve reported in Version 50 of these tables.

<sup>j</sup>Spectral response and current–voltage curve reported in Version 54 of these tables.

<sup>k</sup>Spectral response and current–voltage curve reported in Version 60 of these tables.

<sup>l</sup>Stabilized by 1000 h exposure to 1 sun light at 50°C.

<sup>m</sup>Initial performance. Han et al.<sup>23</sup> and Yang and You<sup>24</sup> review the stability of similar devices.

<sup>n</sup>Initial efficiency. Krašovec et al.<sup>25</sup> review the stability of similar devices.

<sup>a</sup>Spectral response and current–voltage curve reported in Version 41 of these tables.

<sup>b</sup>Spectral response and current–voltage curve reported in Version 46 of these tables.

<sup>c</sup>Spectral response and current–voltage curve reported in Version 43 of these tables.

<sup>f</sup>Initial performance. Tanembaum et al.,<sup>26</sup> Krebs,<sup>27</sup> and Jorgensen et al.<sup>28</sup> review the stability of similar devices.

<sup>s</sup>Spectral response and current–voltage curve reported in Version 55 of these tables.

**TABLE 2** “Notable exceptions” for single-junction cells and submodules: “Top dozen” confirmed results, not class records, measured under the global AM1.5 spectrum (1000 W m<sup>−2</sup>) at 25°C (IEC 60904-3: 2008 or ASTM G-173-03 global)

Classification	Efficiency (%)	Area (cm <sup>2</sup> )	V <sub>oc</sub> (V)	J <sub>sc</sub> (mA/cm <sup>2</sup> )	Fill factor (%)	Test centre (date)	Description
<i>Cells (silicon)</i>							
Si (crystalline)	25.0 ± 0.5	4.00 (da)	0.706	42.7 <sup>a</sup>	82.8	Sandia (3/99)	UNSW, p-type PERC <sup>29</sup>
Si (crystalline)	25.8 ± 0.5 <sup>b</sup>	4.008 (da)	0.7241	42.87	83.1	FhG-ISE (7/17)	FhG-ISE, n-type TOPCon <sup>30</sup>
Si (crystalline)	26.0 ± 0.5 <sup>b</sup>	4.015 (da)	0.7323	42.05 <sup>d</sup>	84.3	FhG-ISE (11/19)	FhG-ISE, p-type TOPCon
Si (crystalline)	26.7 ± 0.5	79.0 (da)	0.738	42.65 <sup>f</sup>	84.9	AIST (3/17)	Kaneka, n-type rear IBC <sup>32</sup>
Si (crystalline)	26.1 ± 0.3 <sup>b</sup>	3.9857 (da)	0.7266	42.62 <sup>e</sup>	84.3	ISFH (2/18)	ISFH, p-type rear IBC <sup>31</sup>
Si (large crystalline)	24.0 ± 0.3 <sup>g</sup>	244.59 (t)	0.6940	41.58 <sup>h</sup>	83.3	ISFH (7/19)	LONGi, p-type PERC <sup>33</sup>
Si (large crystalline)	25.3 ± 0.4 <sup>i</sup>	268.0 (t)	0.7214	42.07 <sup>j</sup>	83.4	ISFH (11/21)	Jinko, n-type TOPCon <sup>34</sup>
<b>Si (large crystalline)</b>	<b>26.6 ± 0.4<sup>k</sup></b>	<b>274.1 (t)</b>	<b>0.7513</b>	<b>41.30<sup>l</sup></b>	<b>85.6</b>	<b>ISFH (10/22)</b>	<b>LONGi, p-type HJT<sup>35</sup></b>
Si (large crystalline)	26.6 ± 0.5	179.74 (da)	0.7403	42.5 <sup>f</sup>	84.7	FhG-ISE (11/16)	Kaneka, n-type rear IBC <sup>32</sup>
<i>Cells (III–V)</i>							
GaInP	22.0 ± 0.3 <sup>b</sup>	0.2502 (ap)	1.4695	16.63 <sup>m</sup>	90.2	NREL (1/19)	NREL, rear HJ, strained AlInP <sup>36</sup>
<i>Cells (chalcogenide)</i>							
CdTe (thin-film)	22.1 ± 0.5	0.4798 (da)	0.8872	31.69 <sup>n</sup>	78.5	Newport (11/15)	First Solar on glass <sup>37</sup>
CZTSSe (thin-film)	13.0 ± 0.1	0.1072 (ap)	0.5294	33.58 <sup>o</sup>	72.9	NREL (6/21)	NJUPT (10% Ag) <sup>38</sup>
CZTS (thin-film)	11.0 ± 0.2	0.2339 (da)	0.7306	21.74 <sup>f</sup>	69.3	NREL (3/17)	UNSW on glass <sup>39</sup>
<i>Cells (other)</i>							
Perovskite (thin-film)	25.7 ± 0.8 <sup>p,q</sup>	0.09597 (ap)	1.1790	25.80 <sup>j</sup>	84.6	Newport (11/21)	UNIST Ulsan <sup>40</sup>
Organic (thin-film)	18.2 ± 0.2 <sup>r</sup>	0.0322 (da)	0.8965	25.72 <sup>h</sup>	78.9	NREL (10/20)	SJTU Shanghai/Beihang U.
Dye sensitised	12.25 ± 0.4 <sup>s</sup>	0.0963 (ap)	1.0203	15.17 <sup>d</sup>	79.1	Newport (8/19)	EPFL <sup>41</sup>

Abbreviations: AIST, Japanese National Institute of Advanced Industrial Science and Technology; (ap), aperture area; CIGSSe, CuInGaSSe; CZTSSe, Cu<sub>2</sub>ZnSnS<sub>4-x</sub>Se<sub>x</sub>; CZTS, Cu<sub>2</sub>ZnSnS<sub>4</sub>; (da), designated illumination area; DS, directionally solidified (including mono cast and multicrystalline); FhG-ISE, Fraunhofer-Institut für Solare Energiesysteme; ISFH, Institute for Solar Energy Research, Hamelin; NREL, National Renewable Energy Laboratory; (t), total area.

<sup>a</sup>Spectral response reported in Version 36 of these tables.

<sup>b</sup>Not measured at an external laboratory.

<sup>c</sup>Spectral response and current–voltage curves reported in Version 51 of these tables.

<sup>d</sup>Spectral response and current–voltage curves reported in Version 55 of these tables.

<sup>e</sup>Spectral response and current–voltage curve reported in Version 52 of these tables.

<sup>f</sup>Spectral response and current–voltage curves reported in Version 50 of these tables.

<sup>g</sup>Contacting: front: 12BB, busbar resistance neglected; rear: fully metallized, full area contacting.

<sup>h</sup>Spectral response and current–voltage curves reported in Version 57 of these tables.

<sup>i</sup>Contacting: front: OBB, grid resistance neglecting; rear: 9BB, full area contacting, highly reflective chuck.

<sup>j</sup>Spectral response and current–voltage curves reported in the Version 60 of these tables.

<sup>k</sup>Contacting: front: busbar resistance neglecting contacting; rear: 9BB, grid resistance neglecting contacting, gold plated chuck.

<sup>l</sup>Spectral response and current–voltage curve reported in present version of these tables.

<sup>m</sup>Spectral response and current–voltage curve reported in Version 54 of these tables.

<sup>n</sup>Spectral response and/or current–voltage curves reported in Version 46 of these tables.

<sup>o</sup>Spectral response and current–voltage curves reported in Version 59 of these tables.

<sup>p</sup>Stability not investigated. Han et al.<sup>23</sup> and Yang and You<sup>24</sup> document stability of similar devices.

<sup>q</sup>Measured using 10-point IV sweep with constant voltage bias until current change rate <0.07%/min.

<sup>r</sup>Long-term stability not investigated. Tanembaum et al.,<sup>26</sup> Krebs,<sup>27</sup> and Jorgensen et al.<sup>28</sup> document stability of similar devices.

<sup>s</sup>Long-term stability not investigated. Krašovec et al.<sup>25</sup> document stability of similar devices.

**TABLE 3** Confirmed multiple-junction terrestrial cell and submodule efficiencies measured under the global AM1.5 spectrum (1000 W/m<sup>2</sup>) at 25°C (IEC 60904-3: 2008 or ASTM G-173-03 global)

Classification	Efficiency (%)	Area (cm <sup>2</sup> )	Voc (V)	Jsc (mA/cm <sup>2</sup> )	Fill factor (%)	Test centre (date)	Description
<i>III-V Multijunctions</i>							
5 junction cell (bonded)	38.8 ± 1.2	1.021 (ap)	4.767	9.564	85.2	NREL (7/13)	Spectrolab, 2-terminal
(2.17/1.68/1.40/1.06/.73 eV)							
InGaP/GaAs/InGaAs	37.9 ± 1.2	1.047 (ap)	3.065	14.27 <sup>a</sup>	86.7	AIST (2/13)	Sharp, 2 term. <sup>42</sup>
GaInP/GaAs (monolithic)	32.8 ± 1.4	1.000 (ap)	2.568	14.56 <sup>b</sup>	87.7	NREL (9/17)	LG Electronics, 2 term.
<i>Multijunctions with c-Si</i>							
GaInP/GaInAsP/Si (wafer bonded)	35.9 ± 1.3 <sup>c</sup>	3.987 (ap)	3.248	13.11 <sup>d</sup>	84.3	FhG-ISE (4/20)	Fraunhofer ISE, 2-term. <sup>43</sup>
GaInP/GaAs/Si (mech. stack)	35.9 ± 0.5 <sup>c</sup>	1.002 (da)	2.52/0.681	13.6/11.0	87.5/78.5	NREL (2/17)	NREL/CSEM/EPFL, 4-term. <sup>44</sup>
GaInP/GaAs/Si (monolithic)	25.9 ± 0.9 <sup>c</sup>	3.987 (ap)	2.647	12.21 <sup>e</sup>	80.2	FhG-ISE (6/20)	Fraunhofer ISE, 2-term. <sup>45</sup>
GaAsP/Si (monolithic)	23.4 ± 0.3	1.026 (ap)	1.732	17.34 <sup>f</sup>	77.7	NREL (5/20)	OSU/UNSW/SolAero, 2-term <sup>46</sup>
GaAs/Si (mech. stack)	32.8 ± 0.5 <sup>c</sup>	1.003 (da)	1.09/0.683	28.9/11.1 <sup>g</sup>	85.0/79.2	NREL (12/16)	NREL/CSEM/EPFL, 4-term. <sup>44</sup>
<b>Perovskite/Si</b>	<b>31.3 ± 0.3<sup>h</sup></b>	<b>1.1677 (da)</b>	<b>1.9131</b>	<b>20.47<sup>i</sup></b>	<b>79.8</b>	<b>NREL (6/22)</b>	<b>EPFL/CSEM, 2-term.<sup>47</sup></b>
GaInP/GaInAs/Ge; Si (spectral split minimodule)	34.5 ± 2.0	27.83 (ap)	2.66/0.65	13.1/9.3	85.6/79.0	NREL (4/16)	UNSW/Azur/Trina, 4-term. <sup>48</sup>
<i>Other Multijunctions</i>							
Perovskite/CIGS	24.2 ± 0.7 <sup>h</sup>	1.045 (da)	1.768	19.24 <sup>f</sup>	72.9	FhG-ISE (1/20)	HZB, 2-terminal <sup>49</sup>
Perovskite/perovskite	26.4 ± 0.7 <sup>h</sup>	1.044 (da)	2.118	15.22 <sup>p</sup>	82.6	JET (3/22)	SichuanU/EMPA, 2-term. <sup>50</sup>
<b>Perovskite/perovskite (minimodule)</b>	<b>24.5 ± 0.6<sup>h</sup></b>	<b>20.25 (da)</b>	<b>2.157</b>	<b>14.86<sup>i</sup></b>	<b>77.5</b>	<b>JET (6/22)</b>	<b>Nanjing/Renshine, 2-term.<sup>51</sup></b>
a-Si/nc-Si/nc-Si (thin-film)	14.0 ± 0.4 <sup>ic</sup>	1.045 (da)	1.922	9.94 <sup>k</sup>	73.4	AIST (5/16)	AIST, 2-term. <sup>52</sup>
a-Si/nc-Si (thin-film cell)	12.7 ± 0.4 <sup>ic</sup>	1.000 (da)	1.342	13.45 <sup>l</sup>	70.2	AIST (10/14)	AIST, 2-term. <sup>53</sup>
<i>"Notable Exceptions"</i>							
GaInP/GaAs (mqw)	32.9 ± 0.5 <sup>c</sup>	0.250 (ap)	2.500	15.36 <sup>m</sup>	85.7	NREL (1/20)	NREL/UNSW, multiple QW
GaInP/GaAs/GaInAs	37.8 ± 1.4	0.998 (ap)	3.013	14.60 <sup>m</sup>	85.8	NREL (1/18)	Microlink (ELO) <sup>54</sup>
GaInP/GaAs (mqw)/GaInAs	39.5 ± 0.5 <sup>c</sup>	0.242 (ap)	2.997	15.44 <sup>n</sup>	85.3	NREL (9/21)	NREL, multiple QW
6 junction (monolithic) (2.19/1.76/1.45/1.19/.97/.7 eV)	39.2 ± 3.2 <sup>c</sup>	0.247 (ap)	5.549	8.457 <sup>o</sup>	83.5	NREL (11/18)	NREL, inv. metamorphic <sup>55</sup>
GaInP/AlGaAs/CIGS	28.1 ± 1.2 <sup>c</sup>	0.1386 (da)	2.952	11.72 <sup>d</sup>	81.1	AIST (1/21)	AIST/FhG-ISE, 2-term. <sup>56</sup>
Perovskite/Si (large)	26.8 ± 1.2 <sup>h</sup>	274.22 (t)	1.891	17.84 <sup>p</sup>	79.4	FhG-ISE (11/21)	Oxford PV, 2-term.
Perovskite/perovskite	28.0 ± 0.6 <sup>h</sup>	0.0495 (da)	2.125	16.42 <sup>p</sup>	80.3	JET (12/21)	Nanjing U, 2-term. <sup>51</sup>
Perovskite/organic	23.4 ± 0.8 <sup>h</sup>	0.0552 (da)	2.136	14.56 <sup>p</sup>	75.6	JET (3/22)	NUS/SERIS, 2-term. <sup>57</sup>

Abbreviations: AIST, Japanese National Institute of Advanced Industrial Science and Technology; (ap), aperture area; a-Si, amorphous silicon/hydrogen alloy; (da), designated illumination area; FhG-ISE, Fraunhofer Institut für Solare Energiesysteme; nc-Si, nanocrystalline or microcrystalline silicon; (t), total area.

<sup>a</sup>Spectral response and current–voltage curve reported in Version 42 of these tables.

<sup>b</sup>Spectral response and current–voltage curve reported in the Version 51 of these tables.

<sup>c</sup>Not measured at an external laboratory.

<sup>d</sup>Spectral response and current–voltage curve reported in Version 58 of these tables.

<sup>e</sup>Spectral response and current–voltage curve reported in Version 57 of these tables.

<sup>f</sup>Spectral response and current–voltage curve reported in Version 56 of these tables.

<sup>g</sup>Spectral response and current–voltage curve reported in Version 52 of these tables.

<sup>h</sup>Initial efficiency. Han et al.<sup>23</sup> and Yang and You<sup>24</sup> review the stability of similar perovskite-based devices.

<sup>i</sup>Spectral response and current–voltage curves reported in the present version of these tables.

<sup>j</sup>Stabilized by 1000 h exposure to 1 sun light at 50°C.

<sup>k</sup>Spectral response and current–voltage curve reported in Version 49 of these tables.

<sup>l</sup>Spectral responses and current–voltage curve reported in Version 45 of these tables.

<sup>m</sup>Spectral response and current–voltage curve reported in Version 53 of these tables.

<sup>n</sup>Spectral response and current–voltage curves reported in Version 59 of these tables.

<sup>o</sup>Spectral response and current–voltage curve reported in Version 54 of these tables.

<sup>p</sup>Spectral response and current–voltage curve reported in Version 60 of these tables.

**TABLE 4** Confirmed non-concentrating terrestrial module efficiencies measured under the global AM1.5 spectrum (1000 W/m<sup>2</sup>) at a cell temperature of 25°C (IEC 60904-3: 2008 or ASTM G-173-03 global)

Classification	Effic. (%)	Area (cm <sup>2</sup> )	V <sub>oc</sub> (V)	I <sub>sc</sub> (A)	FF (%)	Test centre (date)	Description
Si (crystalline)	24.4 ± 0.5	13,177 (da)	79.5	5.04 <sup>a</sup>	80.1	AIST (9/16)	Kaneka (108 cells) <sup>32</sup>
Si (multicrystalline)	20.4 ± 0.3	14,818 (ap)	39.90	9.833 <sup>b</sup>	77.2	FhG-ISE (10/19)	Hanwha Q Cells (60 cells) <sup>58</sup>
GaAs (thin-film)	25.1 ± 0.8	866.45 (ap)	11.08	2.303 <sup>c</sup>	85.3	FhG-ISE (11/17)	Alta Devices <sup>59</sup>
CIGS (Cd-free)	19.2 ± 0.5	841 (ap)	48.0	0.456 <sup>c</sup>	73.7	AIST (1/17)	Solar Frontier (70 cells) <sup>60</sup>
CdTe (thin-film)	19.5 ± 1.4	23,582 (da)	227.9	2.622 <sup>d</sup>	76.8	NREL (9/21)	First Solar <sup>61</sup>
a-Si/nc-Si (tandem)	12.3 ± 0.3 <sup>e</sup>	14,322 (t)	280.1	0.902 <sup>f</sup>	69.9	ESTI (9/14)	TEL Solar, Trubbach Labs <sup>62</sup>
Perovskite	17.9 ± 0.5 <sup>g</sup>	804 (da)	58.7	0.323 <sup>h</sup>	76.1	AIST (1/20)	Panasonic (55 cells) <sup>63</sup>
Organic	8.7 ± 0.3 <sup>i</sup>	802 (da)	17.47	0.569 <sup>j</sup>	70.4	AIST (5/14)	Toshiba <sup>64</sup>
<b>Multijunction</b>							
InGaP/GaAs/InGaAs	32.65 ± 0.7	965 (da)	24.30	1.520 <sup>d</sup>	85.3	AIST (2/22)	Sharp (40 cells; 8 series) <sup>65</sup>
<b>“Notable Exception”</b>							
CIGS (large)	18.6 ± 0.6	10,858 (ap)	58.00	4.545 <sup>b</sup>	76.8	FhG-ISE (10/19)	Miasole <sup>66</sup>

Abbreviations: (ap), aperture area; a-Si, amorphous silicon/hydrogen alloy; a-SiGe, amorphous silicon/germanium/hydrogen alloy; CIGSS, CuInGaSSe; (da), designated illumination area; Effic., efficiency; FF, fill factor; nc-Si, nanocrystalline or microcrystalline silicon; (t), total area.

<sup>a</sup>Spectral response and current voltage curve reported in Version 49 of these tables.

<sup>b</sup>Spectral response and current–voltage curve reported in Version 55 of these tables.

<sup>c</sup>Spectral response and current–voltage curve reported in Version 50 or 51 of these tables.

<sup>d</sup>Spectral response and current–voltage curve reported in Version 60 of these tables.

<sup>e</sup>Stabilised at the manufacturer to the 2% level following IEC procedure of repeated measurements.

<sup>f</sup>Spectral response and/or current–voltage curve reported in Version 46 of these tables.

<sup>g</sup>Initial performance. Yang and You<sup>24</sup> and Krašovec et al.<sup>25</sup> review the stability of similar devices.

<sup>h</sup>Spectral response and current–voltage curve reported in Version 57 of these tables.

<sup>i</sup>Initial performance. Green,<sup>29</sup> Krebs,<sup>27</sup> and Jorgensen et al.<sup>28</sup> review the stability of similar devices.

<sup>j</sup>Spectral response and current–voltage curve reported in Version 45 of these tables.

approaches and to clarify the corresponding measurement conditions, an unambiguous denotation was introduced and used in the present version of these tables.

Table results are reported for cells and modules made from different semiconductors and for subcategories within each semiconductor grouping (e.g., crystalline, polycrystalline or directionally solidified and thin film). From Version 36 onwards, spectral response information is included (when possible) in the form of a plot

of the external quantum efficiency (EQE) versus wavelength, either as absolute values or normalised to the peak measured value. Current–voltage (IV) curves have also been included where possible from Version 38 onwards.

Highest confirmed “one sun” cell and module results are reported in Tables 1–4. Any changes in the tables from those previously published<sup>1</sup> are set in bold type. In most cases, a literature reference is provided that describes either the result reported or a similar result

**TABLE 5** Terrestrial concentrator cell and module efficiencies measured under the ASTM G-173-03 direct beam AM1.5 spectrum at a cell temperature of 25°C (except where noted for the hybrid and luminescent modules)

Classification	Effic. (%)	Area (cm <sup>2</sup> )	Intensity <sup>a</sup> (suns)	Test centre (date)	Description
<b>Single cells</b>					
GaAs	30.8 ± 1.9 <sup>b,c</sup>	0.0990 (da)	61	NREL (1/22)	NREL, 1 junction (1J)
Si	27.6 ± 1.2 <sup>d</sup>	1.00 (da)	92	FhG-ISE (11/04)	Amonix back-contact <sup>67</sup>
CIGS (thin-film)	23.3 ± 1.2 <sup>b,e</sup>	0.09902 (ap)	15	NREL (3/14)	NREL <sup>68</sup>
<b>Multijunction cells</b>					
AlGaInP/AlGaAs/GaAs/GaInAs(3) (2.15/1.72/1.41/1.17/0.96/0.70 eV)	47.1 ± 2.6 <sup>b,f</sup>	0.099 (da)	143	NREL (3/19)	NREL, 6J inv. metamorphic <sup>55</sup>
GaInP/GaInAs; GaInAsP/GaInAs	47.6 ± 2.6 <sup>b,g</sup>	0.0452 (da)	665	FhG-ISE (5/22)	FhG-ISE 4J bonded <sup>69</sup>
GaInP/GaAs/GaInAs/GaInAs	45.7 ± 2.3 <sup>b,h</sup>	0.09709 (da)	234	NREL (9/14)	NREL, 4J monolithic <sup>70</sup>
InGaP/GaAs/InGaAs	44.4 ± 2.6 <sup>i</sup>	0.1652 (da)	302	FhG-ISE (4/13)	Sharp, 3J inverted metamorphic <sup>71</sup>
GaInAsP/GaInAs	35.5 ± 1.2 <sup>b,j</sup>	0.10031 (da)	38	NREL (10/17)	NREL 2-junction (2J) <sup>72</sup>
<b>Minimodule</b>					
GaInP/GaAs; GaInAsP/GaInAs	43.4 ± 2.4 <sup>b,k</sup>	18.2 (ap)	340 <sup>l</sup>	FhG-ISE (7/15)	Fraunhofer ISE 4J (lens/cell) <sup>73</sup>
<b>Submodule</b>					
GaInP/GaInAs/Ge; Si	40.6 ± 2.0 <sup>k</sup>	287 (ap)	365	NREL (4/16)	UNSW 4J split spectrum <sup>74</sup>
<b>Modules</b>					
Si	20.5 ± 0.8 <sup>b</sup>	1875 (ap)	79	Sandia (4/89) <sup>l</sup>	Sandia/UNSW/ENTECH (12 cells) <sup>75</sup>
Three Junction (3J)	35.9 ± 1.8 <sup>m</sup>	1,092 (ap)	N/A	NREL (8/13)	Amonix <sup>76</sup>
Four Junction (4J)	38.9 ± 2.5 <sup>n</sup>	812.3 (ap)	333	FhG-ISE (4/15)	Soitec <sup>77</sup>
<b>Hybrid module<sup>o</sup></b>					
4-Junction (4J)/bifacial c-Si	34.2 ± 1.9 <sup>b,o</sup>	1,088 (ap)	CPV/PV	FhG-ISE (9/19)	FhG-ISE (48/8 cells; 4T) <sup>78</sup>
<b>“Notable exceptions”</b>					
Si (large area)	21.7 ± 0.7	20.0 (da)	11	Sandia (9/90) <sup>l</sup>	UNSW laser grooved <sup>79</sup>
Luminescent Minimodule <sup>o</sup>	7.1 ± 0.2	25 (ap)	2.5 <sup>p</sup>	ESTI (9/08)	ECN Petten, GaAs cells <sup>80</sup>
4J Minimodule	41.4 ± 2.6 <sup>b</sup>	121.8 (ap)	230	FhG-ISE (9/18)	FhG-ISE, 10 cells <sup>81</sup>

Note: Following the normal convention, efficiencies calculated under this direct beam spectrum neglect the diffuse sunlight component that would accompany this direct spectrum. These direct beam efficiencies need to be multiplied by a factor estimated as 0.8746 to convert to thermodynamic efficiencies.<sup>82</sup>

Abbreviations: (ap), aperture area; CIGS, CuInGaSe<sub>2</sub>; (da), designated illumination area; Effic., efficiency; FhG-ISE, Fraunhofer-Institut für Solare Energiesysteme; NREL, National Renewable Energy Laboratory.

<sup>a</sup>One sun corresponds to direct irradiance of 1000 W m<sup>-2</sup>.

<sup>b</sup>Not measured at an external laboratory.

<sup>c</sup>Spectral response and current-voltage curve reported in Version 60 of these tables.

<sup>d</sup>Measured under a low aerosol optical depth spectrum similar to ASTM G-173-03 direct.<sup>83</sup>

<sup>e</sup>Spectral response and current-voltage curve reported in Version 44 of these tables.

<sup>f</sup>Spectral response and current-voltage curve reported in Version 54 of these tables.

<sup>g</sup>Spectral response and current-voltage curve reported in the present version of these tables.

<sup>h</sup>Spectral response and current-voltage curve reported in Version 46 of these tables.

<sup>i</sup>Spectral response and current-voltage curve reported in Version 42 of these tables.

<sup>j</sup>Spectral response and current-voltage curve reported in Version 51 of these tables.

<sup>k</sup>Determined at IEC 62670-1 CSTC reference conditions.

<sup>l</sup>Recalibrated from original measurement.

<sup>m</sup>Referenced to 1000 W/m<sup>2</sup> direct irradiance and 25°C cell temperature using the prevailing solar spectrum and an in-house procedure for temperature translation.

<sup>n</sup>Measured under IEC 62670-1 reference conditions following the current IEC power rating draft 62670-3.

<sup>o</sup>Thermodynamic efficiency. Hybrid and luminescent modules measured under the ASTM G-173-03 or IEC 60904-3: 2008 global AM1.5 spectrum at a cell temperature of 25°C.

The hybrid module was a 4-terminal module with external dual-axis tracking. Power rating of CPV follows IEC 62670-3 standard, front power rating of flat plate PV based on IEC 60904-3, 60904-5, 60904-7, and 60904-10 and 60891 with modified current translation approach; rear power rating of flat plate PV based on IEC TS 60904-1-2 and 60891.

<sup>p</sup>Geometric concentration.



(readers identifying improved references are welcome to submit to the lead author). Table 1 summarises the best-reported measurements for “one-sun” (non-concentrator) single-junction cells and submodules.

Table 2 contains what might be described as “notable exceptions” for “one-sun” single-junction cells and submodules in the above category. While not conforming to the requirements to be recognised as a class record, the devices in Table 2 have notable characteristics that will be of interest to sections of the photovoltaic community, with entries based on their significance and timeliness. To encourage discrimination, the table is limited to nominally 12 entries with the present authors having voted for their preferences for inclusion. Readers who have suggestions of notable exceptions for inclusion into this or subsequent tables are welcome to contact any of the authors with full details. Suggestions conforming to the guidelines will be included on the voting list for a future issue.

Table 3 was first introduced in Version 49 of these tables and summarises the growing number of cell and submodule results involving high efficiency, one-sun multiple-junction devices (previously reported in Table 1). Table 4 shows the best results for one-sun modules, both single- and multiple-junction, while Table 5 shows the best results for concentrator cells and concentrator modules. A small number of “notable exceptions” are also included in Tables 3 to 5.

## 2 | NEW RESULTS

Six new results are reported in the present version of these tables. The first new result in Table 1 (“one-sun cells and submodules”) is 26.8% total area efficiency for a large area silicon cell using the silicon heterojunction (HJT) approach, fabricated on an M6 wafer (274 cm<sup>2</sup>) by LONGi Solar<sup>3</sup> and measured by the Institute für Solarenergieforschung (ISFH). This was a monofacial cell measured on a gold-plated brass chuck with frontside busbar and rearside grid resistance

neglecting contacting.<sup>1</sup> The result improves upon the 26.3% HJT result also from LONGi on an M6 wafer reported in Version 59 of these tables and a further improvement to 26.5% reported in June 2022. In September, Sundrive Solar Pty Ltd reported an intermediate HJT result of 26.4% also confirmed by ISFH, using Cu-plated contacts. These efficiencies are all based on total cell area, and the cells are also much larger than the 26.7% former outright record-holding cell, with this cell result now moved to Table 2 as the highest-performing interdigitated back contact (IBC) cell.

The second new result in Table 1 is 22.4% efficiency for a 26-cm<sup>2</sup> perovskite minimodule<sup>17</sup> (a package of interconnected cells of area <200 cm<sup>2</sup>) fabricated by École Polytechnique Fédérale de Lausanne, Sion campus (EPFL-Sion) in conjunction with the North China Electric Power University (NCEPU) and measured by the Chinese National Photovoltaic Industry Measurement and Testing Center (NPVM), improving on the previous 21.4% result.

There is one new result in Table 2 (one-sun “notable exceptions”). LONGi issued a press release<sup>35</sup> in September 2022 reporting that 26.1% efficiency has been measured by ISFH for a large-area (274 cm<sup>2</sup>) gallium-doped p-type silicon cell using LONGi's silicon heterojunction (HJT) approach. In October, this was further improved to 26.6%, narrowing the gap to the outright n-type cell record. This result was for a bifacial cell, measured on a reflective gold-plated brass chuck with frontside busbar and rearside grid resistance neglecting contacting.<sup>1</sup> This is the highest ever efficiency reported for a cell on a p-type wafer.

There are two new results reported in Table 3 relating to one-sun, multijunction devices, all involving perovskite solar cells in various combinations, demonstrating the strength of this technology notwithstanding concerns re long-term stability and toxicity. The first of these new results is 31.3% efficiency for a 1-cm<sup>2</sup> perovskite/silicon monolithic two-junction, two-terminal device fabricated by EPFL PVLAB/CSEM and measured by the US National Renewable Energy Laboratory (NREL). This is the first perovskite tandem cell to exceed the 30% milestone. The second is 24.5% efficiency measured for a

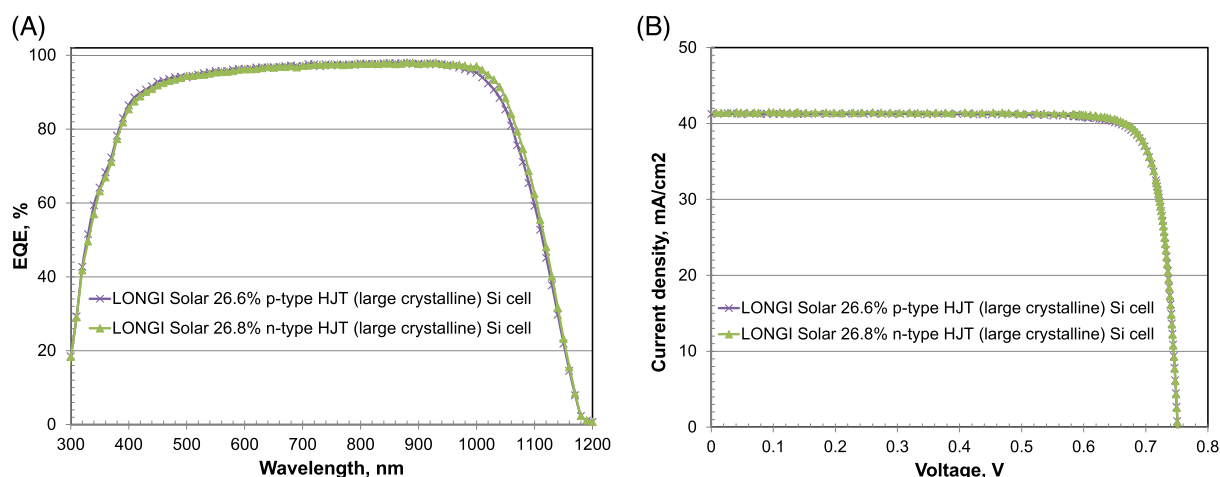


**FIGURE 1** (A) External quantum efficiency (EQE) for the new Si cell results reported in this issue. (B) Corresponding current density–voltage (JV) curves

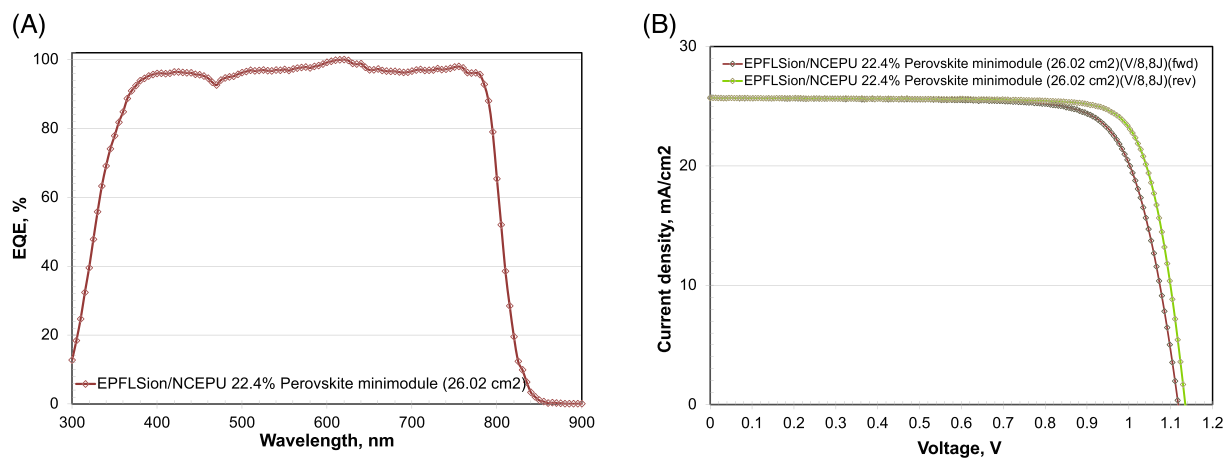


**FIGURE 2** (A) External quantum efficiency (EQE) for the new thin-film cell and minimodule results reported in this issue (some results are normalised). (B) Corresponding current density–voltage (JV) curves

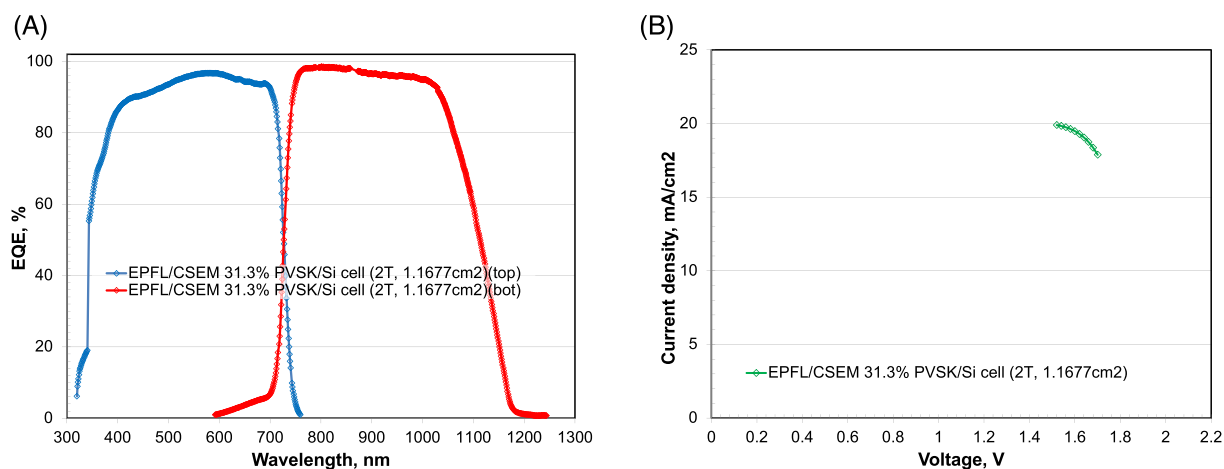


**FIGURE 3** (A) External quantum efficiency (EQE) for the new multijunction cell results reported in this issue (all results are normalised). (B) Corresponding current density–voltage (JV) curves

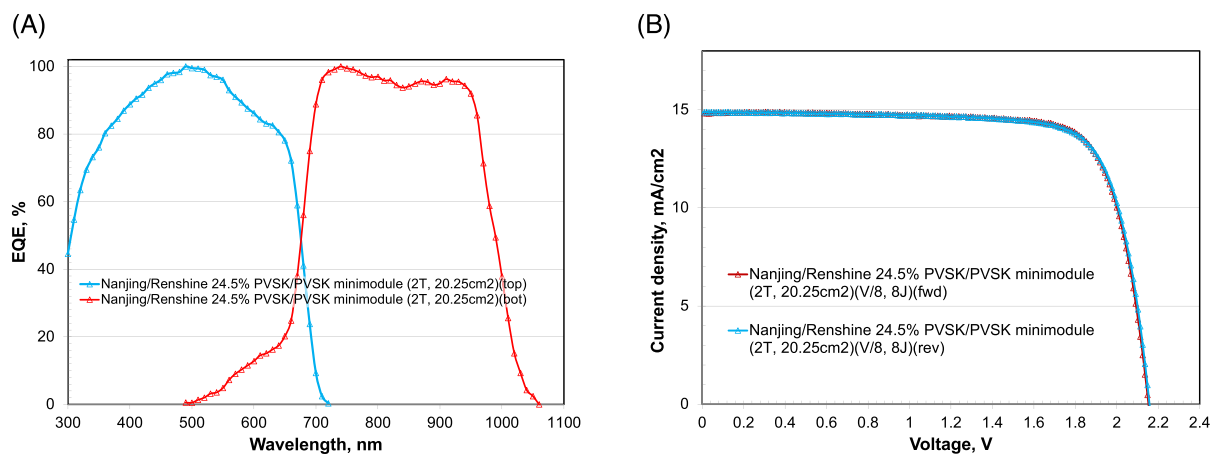


**FIGURE 4** (A) External quantum efficiency (EQE) for the new module results reported in this issue (all results are normalised). (B) Corresponding current density–voltage (JV) curves



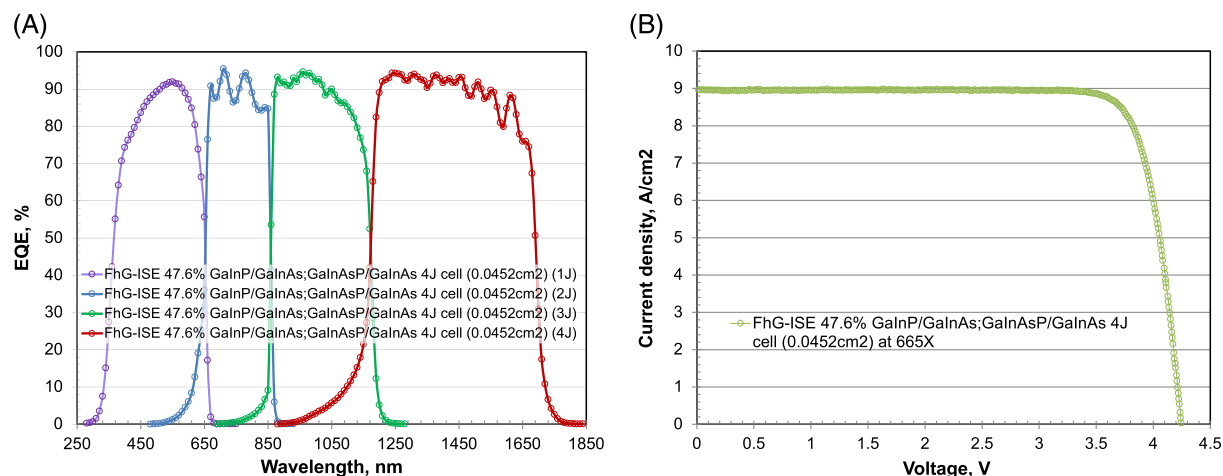


**FIGURE 5** (A) External quantum efficiency (EQE) for the new concentrator cell result reported in this issue. (B) Corresponding current density–voltage (JV) curve

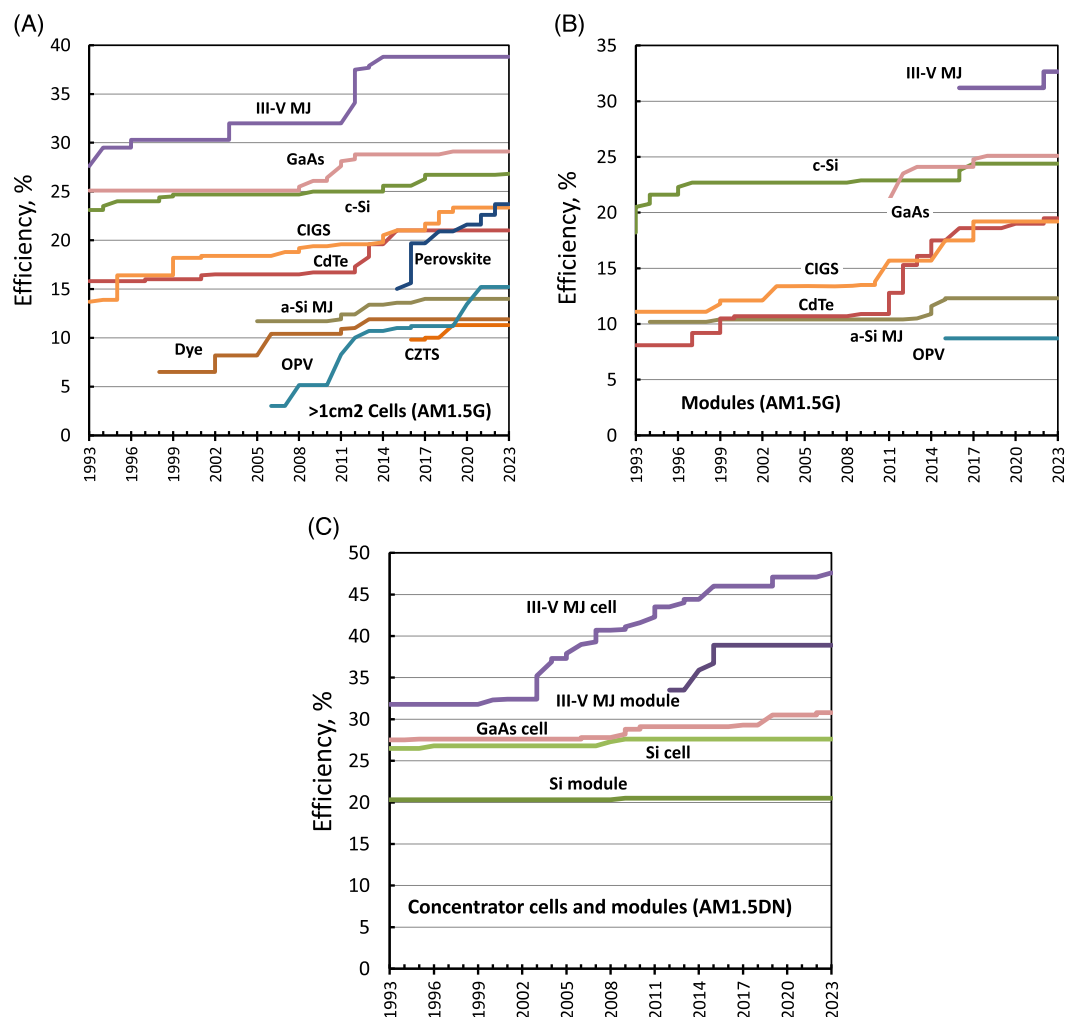


**FIGURE 6** Thirty years of progress: (A) highest confirmed efficiencies for  $\geq 1\text{-cm}^2$  area cells fabricated using the different technologies shown; (B) highest confirmed module results for modules sizes  $\geq 800\text{ cm}^2$ ; (C) highest confirmed concentrator cell and module results

20-cm<sup>2</sup> perovskite/perovskite two-junction, two-terminal minimodule fabricated by Nanjing University and Renshine Solar (Suzhou) Co. Ltd and measured by the Japan Electrical Safety and Environment Technology Laboratories (JET), improving significantly on the team's earlier 21.7% result.

The final new result is in Table 5 (concentrator cells and modules) and documents an improvement to 47.6% efficiency for a four-junction, wafer-bonded concentrator cell based on Group III-V cell technology, with the cell fabricated and measured by the Fraunhofer Institute for Solar Energy Systems (FhG-ISE). This is the highest ever efficiency for a concentrator cell. It should be noted such concentrator cell efficiencies are not directly comparable with the efficiencies of non-concentrating cells, since the former are not true thermodynamic efficiencies (diffuse light that cannot be concentrated is not included into the efficiency definition).

The EQE spectra for the new silicon cells reported in the present issue of these tables are shown in Figure 1A, with Figure 1B showing the current density–voltage (JV) curves for the same devices. Figure 2A,B shows the corresponding EQE and JV curves for the new thin-film cell minimodule results, Figure 3A,B shows these for the new multijunction cell results, and Figure 4A,B show these for the new module results while Figure 5A,B shows these for the new GaAs concentrator cell result.

### 3 | PROGRESS OVER THE LAST 30 YEARS

Figure 6 reports 30 years of progress in confirmed cell and module efficiencies since the first version of these tables was published in 1993. Figure 6A shows the progress with 'one-sun' cells of  $\geq 1\text{-cm}^2$  area. Recent progress with organic, perovskite and CdTe cells has been most notable, with good progress also with CIGS. Figure 6B shows similar progress with photovoltaic modules with CdTe and CIGS being the recent standouts. Figure 6C shows the results for concentrator cells and modules. Impressive progress has been made with monolithic III–V MJ cells where efficiency has been improved from 31.8% to 47.6% over the 30-year period (efficiency, in this case, is boosted relative to results in Figure 6A,B since based on only the direct normal component of the solar spectrum, with the diffuse component neglected in the efficiency calculation as previously mentioned).

### 4 | DISCLAIMER

While the information provided in the tables is provided in good faith, the authors, editors and publishers cannot accept direct responsibility for any errors or omissions.

### ACKNOWLEDGEMENTS

The Australian Centre for Advanced Photovoltaics commenced operation in February 2013 with support from the Australian Government through the Australian Renewable Energy Agency (ARENA). The

Australian Government does not accept responsibility for the views, information or advice expressed herein. The work at NREL was supported by the U.S. Department of Energy under Contract No. DE-AC36-08-GO28308 with the National Renewable Energy Laboratory. The work at AIST was supported in part by the Japanese New Energy and Industrial Technology Development Organisation (NEDO) under the Ministry of Economy, Trade and Industry (METI). Open access publishing facilitated by University of New South Wales, as part of the Wiley - University of New South Wales agreement via the Council of Australian University Librarians.

### DATA AVAILABILITY STATEMENT

The data that support the findings of this study are available from the corresponding author upon reasonable request.

### ORCID

Martin A. Green  <https://orcid.org/0000-0002-8860-396X>

### REFERENCES

- Green MA, Dunlop ED, Hohl-Ebinger J, Yoshita M, Kopidakis N, Hao XJ. Solar cell efficiency tables (Version 60). *Prog Photovolt Res Appl*. 2022;30(7):687–701. doi:10.1002/pip.3595
- Green MA, Emery K, Hishikawa Y, Warta W. Solar cell efficiency tables (Version 33). *Prog Photovolt Res Appl*. 2009;17(1):85–94. doi:10.1002/pip.88
- LONGi once again sets new world record for HJT solar cell efficiency. Press Release, 24 June 2022. <https://www.longi.com/en/news/new-hjt-world-record/>
- Moslehi MM, Kapur P, Kramer J, et al. World-record 20.6% efficiency 156 mm x 156 mm full-square solar cells using low-cost kerfless ultrathin epitaxial silicon & porous silicon lift-off technology for industry-leading high-performance smart PV modules. *PV Asia Pacific Conference (APVIA/PVAP)*, 24 October 2012.
- Keevers MJ, Young TL, Schubert U, Green MA. 10% efficient CSG minimodules. 22nd European Photovoltaic Solar Energy Conference, Milan, September 2007.
- Kayes BM, Nie H, Twist R, et al. 27.6% conversion efficiency, a new record for single-junction solar cells under 1 sun illumination. *Proceedings of the 37th IEEE Photovoltaic Specialists Conference*, 2011.
- Venkatasubramanian R, O'Quinn BC, Hills JS, et al. 18.2% (AM1.5) efficient GaAs solar cell on optical-grade polycrystalline Ge substrate. Conference Record, 25th IEEE Photovoltaic Specialists Conference, Washington, May 1997, 31–36.
- Wanlass M. Systems and methods for advanced ultra-high-performance InP solar cells. US Patent 9,590,131 B2, 7 March 2017.
- Nakamura M, Yamaguchi K, Kimoto Y, Yasaki Y, Kato T, Sugimoto H. Cd-free Cu (In,Ga)(Se,S)<sub>2</sub> thin-film solar cell with a new world record efficacy of 23.35%, 46th IEEE PVSC, Chicago, IL, June 19, 2019. (see also [http://www.solar-frontier.com/eng/news/2019/0117\\_press.html](http://www.solar-frontier.com/eng/news/2019/0117_press.html))
- Diermann R. Avancis claims 19.64% efficiency for CIGS module, PV Magazine International, 4 March 2021. (<https://www.pv-magazine.com/2021/03/04/avancis-claims-19-64-efficiency-for-cigs-module/>)
- First Solar Press Release, First Solar builds the highest efficiency thin film PV cell on record, 5 August 2014.
- [https://en.dgist.ac.kr/site/dgist\\_eng/menu/984.do](https://en.dgist.ac.kr/site/dgist_eng/menu/984.do) (accessed 28 October 2018).
- Yan C, Huang J, Sun K, et al. Cu<sub>2</sub>ZnSn S<sub>4</sub> solar cells with over 10% power conversion efficiency enabled by heterojunction heat treatment. *Nat Energy*. 2018;3(9):764–772. doi:10.1038/s41560-018-0206-0

14. Matsui T, Bidiville A, Sai H, et al. High-efficiency amorphous silicon solar cells: impact of deposition rate on metastability. *Appl Phys Lett*. 2015;106(5):053901. doi:[10.1063/1.4907001](https://doi.org/10.1063/1.4907001)
15. Sai H, Matsui T, Kumagai H, Matsubara K. Thin-film microcrystalline silicon solar cells: 11.9% efficiency and beyond. *Appl Phys Express*. 2018;11(2):022301. doi:[10.7567/APEX.11.022301](https://doi.org/10.7567/APEX.11.022301)
16. Peng J, Walter D, Ren Y, et al. Nanoscale localized contacts for high fill factors in polymer-passivated perovskite solar cells. *Science*. 2021; 371(6527):390-395. doi:[10.1126/science.abb8687](https://doi.org/10.1126/science.abb8687)
17. Ding B, Yi Zhang Y, Yong Ding Y, et al. Development of efficient and stable perovskite solar cells and modules. Fifth International Conference on Materials & Environmental Science (ICMES-2022), June 09–12, 2022, Saïdia, Morocco.
18. Han L, Fukui A, Chiba Y, et al. Integrated dye-sensitized solar cell module with conversion efficiency of 8.2%. *Appl Phys Lett*. 2009; 94(1):013305. doi:[10.1063/1.3054160](https://doi.org/10.1063/1.3054160)
19. Komiya R, Fukui A, Murofushi N, Koide N, Yamanaka R, Katayama H. Improvement of the conversion efficiency of a monolithic type dye-sensitized solar cell module. Technical Digest, 21st International Photovoltaic Science and Engineering Conference, Fukuoka, November 2011; 2C-50-08.
20. Würfel U, Herterich J, List M, et al. A 1 cm<sup>2</sup> organic solar cell with 15.2% certified efficiency: detailed characterization and identification of optimization potential. *Sol RRL*. 2021;5:2000802. doi:[10.1002/solr.202000802](https://doi.org/10.1002/solr.202000802)
21. Fan JY, Liu ZX, Rao J, et al. High-performance organic solar modules via the bilayer-merged-annealing assisted blading coating. *Adv Mater*. 2022;34(28):2110569. doi:[10.1002/adma.202110569](https://doi.org/10.1002/adma.202110569)
22. [https://www.encl.de/fileadmin/user\\_upload/PR\\_opv-record\\_.pdf](https://www.encl.de/fileadmin/user_upload/PR_opv-record_.pdf) (accessed 11 November 2019).
23. Han Y, Meyer S, Dkhissi Y, et al. Degradation observations of encapsulated planar CH<sub>3</sub>NH<sub>3</sub>PbI<sub>3</sub> perovskite solar cells at high temperatures and humidity. *J Mater Chem A*. 2015;3(15):8139-8147. doi:[10.1039/C5TA00358J](https://doi.org/10.1039/C5TA00358J)
24. Yang Y, You J. Make perovskite solar cells stable. *Nature*. 2017; 544(7649):155-156. doi:[10.1038/544155a](https://doi.org/10.1038/544155a)
25. Krašovec UO, Bokalič M, Topič M. Ageing of DSSC studied by electroluminescence and transmission imaging. *Solar Energy Mater Solar Cells*. 2013;117:67-72. doi:[10.1016/j.solmat.2013.05.029](https://doi.org/10.1016/j.solmat.2013.05.029)
26. Tanenbaum DM, Hermenau M, Voroshazi E, et al. The ISOS-3 inter-laboratory collaboration focused on the stability of a variety of organic photovoltaic devices. *RSC Adv*. 2012;2(3):882-893. doi:[10.1039/C1RA00686J](https://doi.org/10.1039/C1RA00686J)
27. Krebs FC (Ed). *Stability and Degradation of Organic and Polymer Solar Cells*. Chichester: Wiley; 2012.
28. Jorgensen M, Norrman K, Gevorgyan SA, Tromholt T, Andreasen B, Krebs FC. Stability of polymer solar cells. *Adv Mater*. 2012;24(5): 580-612. doi:[10.1002/adma.201104187](https://doi.org/10.1002/adma.201104187)
29. Green MA. The passivated emitter and rear cell (PERC): from conception to mass production. *Solar Energy Mater Solar Cells*. 2015;143: 190-197. doi:[10.1016/j.solmat.2015.06.055](https://doi.org/10.1016/j.solmat.2015.06.055)
30. Richter A, Benick J, Feldmann F, Fell A, Hermle M, Glunz SW. n-Type Si solar cells with passivating electron contact: Identifying sources for efficiency limitations by wafer thickness and resistivity variation. *Solar Energy Mater Solar Cells*. 2017;173:96-105. doi:[10.1016/j.solmat.2017.05.042](https://doi.org/10.1016/j.solmat.2017.05.042)
31. Haase F, Klamt C, Schäfer S, et al. Laser contact openings for local poly-Si-metal contacts enabling 26.1%-efficient POLO-IBC solar cells. *Solar Energy Mater Solar Cells*. 2018;186:184-193. doi:[10.1016/j.solmat.2018.06.020](https://doi.org/10.1016/j.solmat.2018.06.020)
32. Yoshikawa K, Kawasaki H, Yoshida W, et al. Silicon heterojunction solar cell with interdigitated back contacts for a photoconversion efficiency over 26%. *Nat Energy*. 2017;2(5):17032. doi:[10.1038/nenergy.2017.32](https://doi.org/10.1038/nenergy.2017.32)
33. Wang Q. Status of crystalline silicon PERC solar cells. NIST/UL Workshop on Photovoltaic Materials Durability, Gaithersburg, MD USA, Dec 12–13, 2019.
34. <https://taiyangnews.info/technology/jinkosolar-record-25-25-efficiency-for-n-type-mono-cell/>
35. LONGi achieves new world record for p-type solar cell efficiency. Press Release: 20 September 2022. <https://www.longi.com/en/news/p-type-hjt-record/>
36. NREL, private communication, 22 May 2019.
37. First Solar Press Release. First Solar achieves yet another cell conversion efficiency world record, 24 February 2016.
38. [http://solar.iphy.ac.cn/en\\_detail.php?id=37673](http://solar.iphy.ac.cn/en_detail.php?id=37673)
39. Sun K, Yan C, Liu F, et al. Beyond 9% efficient kesterite Cu<sub>2</sub>ZnSnS<sub>4</sub> solar cell: fabricated by using Zn<sub>1-x</sub>Cd<sub>x</sub>S buffer layer. *Adv Energy Mater*. 2016;6(12):1600046. doi:[10.1002/aenm.201600046](https://doi.org/10.1002/aenm.201600046)
40. Jeong M, Choi IW, Go EM, et al. Stable perovskite solar cells with efficiency exceeding 24.8% and 0.3-V voltage loss. *Science*. 2020; 369(6511):1615-1620. doi:[10.1126/science.abb7167](https://doi.org/10.1126/science.abb7167)
41. <https://www.epfl.ch/labs/lspm/>; <https://www.epfl.ch/labs/lpi/> (accessed 28 October 2019).
42. Sasaki K, Agui T, Nakaido K, Takahashi N, Onitsuka R, Takamoto T. Proceedings, 9th International Conference on Concentrating Photovoltaics Systems, Miyazaki, Japan 2013.
43. Schygulla P, Müller R, Lackner D, et al. Two-terminal III-V//Si triple-junction solar cell with power conversion efficiency of 35.9% at AM1.5g. *Prog Photovolt Res Appl*. 2022;30(8):869-879. doi:[10.1002/pip.3503](https://doi.org/10.1002/pip.3503)
44. Essig S, Allebé C, Remo T, et al. Raising the one-sun conversion efficiency of III-V/Si solar cells to 32.8% for two junctions and 35.9% for three junctions. *Nat Energy*. 2017;2:17144. doi:[10.1038/nenergy.2017.144](https://doi.org/10.1038/nenergy.2017.144)
45. Feifel M, Lackner D, Schön J, et al. Epitaxial GaInP/GaAs/Si triple-junction solar cell with 25.9% AM1.5g efficiency enabled by transparent metamorphic Al<sub>x</sub>Ga<sub>1-x</sub>As<sub>y</sub>P<sub>1-y</sub> step-graded buffer structures. *Sol RRL*. 2021;5:2000763. doi:[10.1002/solr.202000763](https://doi.org/10.1002/solr.202000763)
46. Grassman TJ, Chmielewski DJ, Carnevale SD, Carlin JA, Ringel SA. GaAs<sub>0.75</sub>P<sub>0.25</sub>/Si dual-junction solar cells grown by MBE and MOCVD. *IEEE J Photovolt*. 2016;6(1):326-331. doi:[10.1109/JPHOTOV.2015.2493365](https://doi.org/10.1109/JPHOTOV.2015.2493365)
47. Bellini E. CSEM, EPFL achieve 31.25% efficiency for tandem perovskite-silicon solar cell. PV Magazine; July 7, 2022. <https://www.pv-magazine.com/2022/07/07/csem-epfl-achieve-31-25-efficiency-for-tandem-perovskite-silicon-solar-cell/>
48. Green MA, Keevers MJ, Concha Ramon B, et al. Improvements in sunlight to electricity conversion efficiency: above 40% for direct sunlight and over 30% for global. Paper 1AP.1.2, European Photovoltaic Solar Energy Conference 2015, Hamburg, September 2015.
49. Jošt M, Köhnen E, Al-Ashouri A, et al. Perovskite/CIGS tandem solar cells: from certified 24.2% toward 30% and beyond. *ACS Energy Lett*. 2022;7(4):1298-1307. doi:[10.1021/acsenergylett.2c00274](https://doi.org/10.1021/acsenergylett.2c00274)
50. Lin R, Xu J, Wei MY, et al. All-perovskite tandem solar cells with improved grain surface passivation. *Nature*. 2022;603(7899):73-78. doi:[10.1038/s41586-021-04372-8](https://doi.org/10.1038/s41586-021-04372-8)
51. Xiao K, Lin YH, Zhang M, et al. Scalable processing for realizing 21.7%-efficient all-perovskite tandem solar modules. *Science*. 2022; 376(6594):762-767. doi:[10.1126/science.abn7696](https://doi.org/10.1126/science.abn7696)
52. Sai H, Matsui T, Koida T, Matsubara K. Stabilized 14.0%-efficient triple-junction thin-film silicon solar cell. *Appl Phys Lett*. 2016;109: 183506. doi:[10.1063/1.4966996](https://doi.org/10.1063/1.4966996)
53. Matsui T, Maejima K, Bidiville A, et al. High-efficiency thin-film silicon solar cells realized by integrating stable a-Si:H absorbers into

- improved device design. *Jpn J Appl Phys.* 2015;54:08KB10. doi:10.7567/JJAP.54.08KB10
54. <http://mldevices.com/index.php/news/> (accessed 28 October 2018).
  55. Geisz JF, Steiner MA, Jain N, et al. Building a six-junction inverted metamorphic concentrator solar cell. *IEEE J Photovoltaics.* 2018;8(2): 626-632. doi:10.1109/JPHOTOV.2017.2778567
  56. Makita K, Kamikawa Y, Mizuno H, et al. III-V//Cu<sub>x</sub>In<sub>1-y</sub>Ga<sub>y</sub>Se<sub>2</sub> multi-junction solar cells with 27.2% efficiency fabricated using modified smart stack technology with Pd nanoparticle array and adhesive material. *Prog Photovolt Res Appl.* 2021;29(8):887-898. doi:10.1002/pip.3398
  57. Chen W, Zhu YD, Xiu JW, et al. Monolithic perovskite/organic tandem solar cells with 23.6% efficiency enabled by reduced voltage losses and optimized interconnecting layer. *Nat Energy.* 2022;7(3): 229-237. doi:10.1038/s41560-021-00966-8
  58. <https://www.hanwha-qcells.com> (accessed 28 October 2019).
  59. Mattos LS, Scully SR, Syfu M, et al. New module efficiency record: 23.5% under 1-sun illumination using thin-film single-junction GaAs solar cells. *Proceedings of the 38th IEEE Photovoltaic Specialists Conference*, 2012.
  60. Sugimoto H. High efficiency and large volume production of CIS-based modules. 40<sup>th</sup> IEEE Photovoltaic Specialists Conference, Denver, June 2014.
  61. <http://www.firstsolar.com/en-AU/-/media/First-Solar/Technical-Documents/Series-6-Datasheets/Series-6-Datasheet.ashx> (accessed 28 October 2019).
  62. Cashmore JS, Apolloni M, Braga A, et al. Improved conversion efficiencies of thin-film silicon tandem (MICROMORPH™) photovoltaic modules. *Solar Energy Mater Solar Cells.* 2016;144:84-95. doi:10.1016/j.solmat.2015.08.022
  63. Higuchi H, Negami T. Largest highly efficient 203 x 203 mm<sup>2</sup> CH<sub>3</sub>NH<sub>3</sub>PbI<sub>3</sub> perovskite solar modules. *Jpn J Appl Phys.* 2018; 57(8S3):08RE11. doi:10.7567/JJAP.57.08RE11
  64. Hosoya M, Oooka H, Nakao H, et al. Organic thin film photovoltaic modules. *Proceedings of the 93rd Annual Meeting of the Chemical Society of Japan* 2013; 21-37.
  65. Sharp Achieves World's Highest<sup>1</sup> Conversion Efficiency of 32.65%<sup>2</sup> in a Lightweight, Flexible, Practically Sized Solar Module. Press Release: June 6, 2022. <https://global.sharp/corporate/news/220606-a.html>
  66. Bheemreddy V, Liu BJJ, Wills A, Murcia CP. Life prediction model development for flexible photovoltaic modules using accelerated damp heat testing. *IEEE 7th World Conf. on Photovoltaic Energy Conversion (WCPEC)* 2018: 1249-1251.
  67. Slade A, Garboushian V. 27.6% efficient silicon concentrator cell for mass production. Technical Digest, 15th International Photovoltaic Science and Engineering Conference, Shanghai, October 2005, 701.
  68. Ward JS, Ramanathan K, Hasoon FS, et al. A 21.5% efficient Cu(In,Ga)Se<sub>2</sub> thin-film concentrator solar cell. *Prog Photovolt Res Appl.* 2002; 10(1):41-46. doi:10.1002/pip.424
  69. Dimroth F, Tibbits TND, Niemeyer M, et al. Four-junction wafer-bonded concentrator solar cells. *IEEE J Photovolt.* 2016;6(1):343-349. doi:10.1109/JPHOTOV.2015.2501729
  70. NREL Press Release NR-4514, 16 December 2014.
  71. Press Release, Sharp Corporation, 31 May 2012. <http://sharp-world.com/corporate/news/120531.html> (accessed 5 June 2013).
  72. Jain N, Schulte KL, Geisz JF, et al. High-efficiency inverted metamorphic 1.7/1.1 eV GaInAsP/GaInAs dual-junction solar cells. *Appl Phys Lett.* 2018;112(5):053905. doi:10.1063/1.5008517
  73. Steiner M, Siefert G, Schmidt T, Wiesenfarth M, Dimroth F, Bett AW. 43% sunlight to electricity conversion efficiency using CPV. *IEEE J Photovolt.* 2016;6(4):1020-1024. doi:10.1109/JPHOTOV.2016.2551460
  74. Green MA, Keevers MJ, Thomas I, Lasich JB, Emery K, King RR. 40% efficient sunlight to electricity conversion. *Prog Photovolt Res Appl.* 2015;23(6):685-691. doi:10.1002/pip.2612
  75. Chiang CJ, Richards EH. A 20% efficient photovoltaic concentrator module. *Conf. Record, 21st IEEE Photovoltaic Specialists Conference*, Kissimmee, May 1990: 861-863.
  76. <http://amonix.com/pressreleases/amonix-achieves-world-record-359-module-efficiency-rating-nrel-4> (accessed 23 October 2013).
  77. van Riesen S, Neubauer M, Boos A, et al. New module design with 4-junction solar cells for high efficiencies. *Proceedings of the 11th Conference on Concentrator Photovoltaic Systems*, 2015.
  78. Martínez JF, Steiner M, Wiesenfarth M, Siefert G, Glunz SW, Dimroth F. Power rating procedure of hybrid CPV/PV bifacial modules. *Prog Photovolt Res Appl.* 2021;29(6):614-629. doi:10.1002/pip.3410
  79. Zhang F, Wenham SR, Green MA. Large area, concentrator buried contact solar cells. *IEEE Trans Electron Devices.* 1995;42(1):144-149. doi:10.1109/16.370024
  80. Slooff LH, Bende EE, Burgers AR, et al. A luminescent solar concentrator with 7.1% power conversion efficiency. *Phys Stat Sol (RRL).* 2008;2(6):257-259. doi:10.1002/pssr.200802186
  81. Steiner M, Wiesenfarth M, Martínez JF, Siefert G, Dimroth F. Pushing energy yield with concentrating photovoltaics. *AIP Conf Proc.* 2019; 2149:060006. doi:10.1063/1.5124199
  82. Mülleijans H, Winter S, Green MA, Dunlop ED. What is the correct efficiency for terrestrial concentrator PV devices? *38th European Photovoltaic Solar Energy Conference*, September 2021 (accepted for presentation).
  83. Gueymard CA, Myers D, Emery K. Proposed reference irradiance spectra for solar energy systems testing. *Solar Energy.* 2002;73(6): 443-467. doi:10.1016/S0038-092X(03)00005-7

**How to cite this article:** Green MA, Dunlop ED, Siefert G, et al. Solar cell efficiency tables (Version 61). *Prog Photovolt Res Appl.* 2023;31(1):3-16. doi:10.1002/pip.3646

## APPENDIX A: AREA DEFINITIONS

The area of the cell or module is a key parameter in determining efficiency. The areas used in the tables conform to one of the three following classifications illustrated in Figure A1:

- i. Total area: The total projected area of the cell or module.

This is the preferred area for reporting of results. For the case of a cell attached to glass, the total area would be the area of the glass sheet. For a module, it would include the area of frames.

- ii. Aperture area: The portion of the total cell or module area that includes all essential components, including active material, busbars, fingers and interconnects.

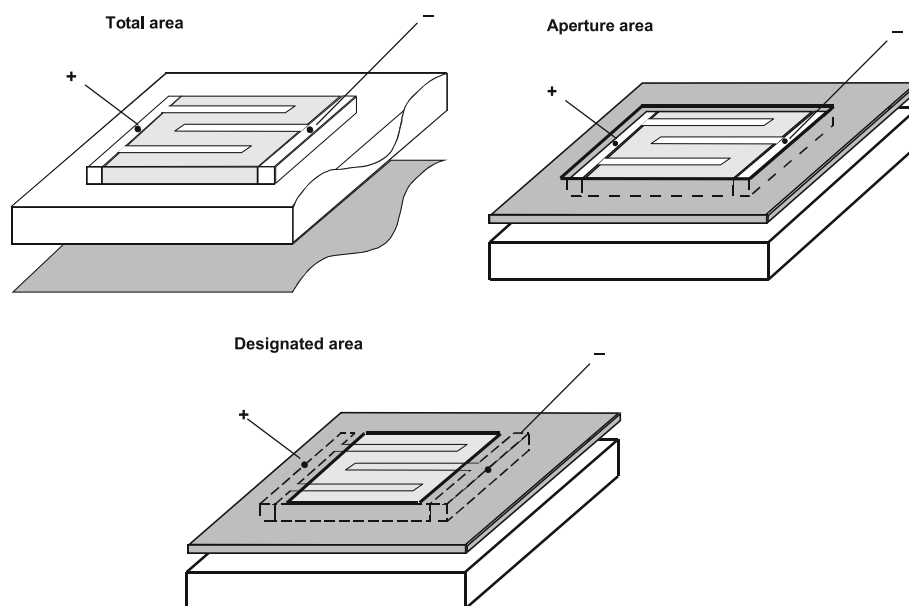


**FIGURE A1** Area classifications: “Total area” (shown grey), “Aperture area” and “Designated illumination area” (the latter two areas are the areas not covered by the mask; masking is not required if the test centre is satisfied that there is no response from the areas shown masked; areas should have a simple non-convoluted geometry such as square, rectangular or circular)

In principle, during testing, illumination is restricted to this portion such as by masking. Such restriction is not essential if the test centre is satisfied that there is no response from light incident outside the assigned aperture area. Note that the assigned aperture area must have a simple geometry, such as square, rectangular or circular.

- iii. Designated illumination area: A portion of the cell or module area from which some cell or module contacting components are excluded. In principle, during testing, illumination is restricted to this portion such as by masking. Such restriction is not essential if the test centre is satisfied that there is no response from light incident outside the assigned designated illumination area. For concentrator cells, cell busbars would lie outside of the area designed for illumination and this area classification would be the most appropriate. For a cell on insulating substrates, cell contacts may lie outside the designated illumination area. For modules, cell string interconnects may lie outside the masked area. Note that the assigned designated illumination area must have a simple geometry, such as square, rectangular or circular.

## APPENDIX B: LIST OF DESIGNATED TEST CENTRES

A list of designated test centres follows. The results from additional ISO/IEC17025 certified centres participating in international round robins involving cells of a similar type to those being reported will also be considered on a case-by-case basis.

### Commonwealth Scientific and Industrial Research Organization (CSIRO)

PV Performance Laboratory  
 10 Murray Dwyer Circuit, Mayfield West, NSW 2304, Australia.  
 Contact: Dr Chris Fell  
 Phone: +61 (2) 4960 6000  
 Email: [chris.fell@csiro.au](mailto:chris.fell@csiro.au)  
 (Perovskite and thin-film solar cells)

### European Solar Test Installation (ESTI)

European Commission – Joint Research Centre, Ispra (VA), Italy.  
 Contact: Dr Ewan Dunlop  
 Telephone: +39 332-789090  
 Facsimile: +39 332-789-268  
 E-mail: [esti.services@jrc.ec.europa.eu](mailto:esti.services@jrc.ec.europa.eu)  
 (Cells and modules)

### Fraunhofer-Institut für Solare Energiesysteme ISE - ISE CalLab

Heidenhofstr. 2, D-79110 Freiburg, Germany.  
 Contacts:  
 Dr Jochen Hohl-Ebinger (terrestrial cells, tandem cells)  
 Phone: +49 (0) 761 4588-5359  
 Facsimile: +49 (0) 761 4588-9359  
 E-mail: [jochen.hohl-ebinger@ise.fraunhofer.de](mailto:jochen.hohl-ebinger@ise.fraunhofer.de)

Dr Gerald Siefer (space and concentrator cells and modules, tandem devices)  
 Phone: +49 (0) 761 4588-5433  
 E-mail: [gerald.siefer@ise.fraunhofer.de](mailto:gerald.siefer@ise.fraunhofer.de)



Frank Neuberger (terrestrial modules),  
Phone: +49 (0) 7614588-5280  
Facsimile: +49 (0) 761 4588-9280  
E-mail: [frank.neuberger@ise.fraunhofer.de](mailto:frank.neuberger@ise.fraunhofer.de)

Institut für Solarenergieforschung GmbH (ISFH)  
Calibration and Test Center (CaTeC), Solar Cells Laboratory,  
Am Ohrberg 1, D-31860 Emmerthal, Germany.  
Contact: Dr Karsten Bothe  
Phone: +49 (0) 5151 999 425  
Facsimile: +49 (0) 5151 999 400  
Mobile: +49 (0) 176 151 999 02  
E-mail: [k.bothe@isfh.de](mailto:k.bothe@isfh.de)  
(Terrestrial cells)

Japan Electrical Safety & Environment Technology Laboratories (JET)  
1-12-28 Motomiya Tsurumi-ku, Yokohama-shi, Kanagawa,  
230-004 Japan.  
Contact: Hiromi Tobita  
Phone: +81-45-570-2073  
Email: [tobita@jet.or.jp](mailto:tobita@jet.or.jp)  
(Terrestrial cells and modules including tandem devices)

National Institute of Advanced Industrial Science and Technology (AIST)  
Central 2, Umezono 1-1-1, Tsukuba, Ibaraki, 305-8568 Japan.  
Contact: Dr Masahiro Yoshita  
Telephone: +81 29-861-3607  
E-mail: [m-yoshita@aist.go.jp](mailto:m-yoshita@aist.go.jp)  
(Terrestrial and concentrator cells and modules including tandem devices)

National Photovoltaic Industry Metrology and Testing Center (NPVM)  
9-3, Pingdong Road, Fuzhou City, Fujian Province, China.  
Contact: Mr Li Jiansheng  
Telephone: +86 0591 8782 5895 or +86 0591 8780 1715  
Facsimile: +86 0591 8782 5895  
Email: [ljs@fjil.net](mailto:ljs@fjil.net)  
(Terrestrial silicon and thin-film solar cells)

National Renewable Energy Laboratory (NREL)  
15013 Denver West Parkway, Golden, CO 80401, USA.  
Contact: Nikos Kopidakis  
Telephone: +1 303-384-6605  
Facsimile: +1 303-384-6604  
E-mail: [niko.kopidakis@nrel.gov](mailto:niko.kopidakis@nrel.gov)  
(Terrestrial, space and concentrator cells and modules including tandem devices)